Available online at www.sciencedirect.com
ScienceDirect
Polymer 48 (2007) 2672–2680
polymer
www.elsevier.com/locate/polymer

Formation and stability of β-structure in biodegradable ultra-high-molecular-weight poly(3-hydroxybutyrate) by infrared, Raman, and quantum chemical calculation studies

Rumi Murakami [a], Harumi Sato [a,b,*], Jiří Dybal [b,c], Tadahisa Iwata [b,d], Yukihiro Ozaki [a,b]

[a] *Department of Chemistry, School of Science and Technology, Kwansei Gakuin University, Sanda 669-1337, Japan*
[b] *Research Center for Environment Friendly Polymers, Kwansei Gakuin University, Sanda 669-1337, Japan*
[c] *Institute of Macromolecular Chemistry, Academy of Science of the Czech Republic, Prague, Czech Republic*
[d] *Department of Biomaterial Sciences, Graduate School of Agricultural and Life Sciences, The University of Tokyo, 1-1-1 Yayoi, Bunkyo-ku, Tokyo 113-8657, Japan*

Received 26 January 2007; received in revised form 26 February 2007; accepted 1 March 2007
Available online 3 March 2007

Abstract

Infrared (IR) and Raman spectra were measured for four kinds of ultra-high-molecular-weight poly[(*R*)-3-hydroxybutyrate] (UHMW-PHB) films: a solvent-cast film, a cold-drawn film, a two-step-drawn film, and a hot-drawn film. Quantum chemical calculations were made for octamer models of UHMW-PHB with a helix conformation (α-form) and a planar zigzag conformation (β-form). Comparison of the results between the Raman spectra of four kinds of films and the quantum chemical calculations of octamer models revealed that only two-step-drawn film yields additional bands at 1735, 966, 935, 908, and 858 cm^{-1} assignable to the β-structure, suggesting that it contains the β-form as well as the α-form. Detailed comparison of the frequencies and intensities of Raman bands between the observed and calculated values for the β-form indicates that the amount of β-form is relatively small and that the β-structure has a less ordered structure. The infrared and Raman spectra of two-step-drawn film also indicate that it has more amorphous parts than other films. When the two-step-drawn film was further heated up to 130 °C and then cooled down to room temperature, the above additional bands due to the β-form disappeared in the Raman spectra, suggesting that the β-form is less stable than α-form.

Keywords: Ultra-high-molecular-weight poly(hydroxybutyrate); β-Form; Raman spectroscopy

1. Introduction

Poly(hydroxyalkanoates) (PHA)s and its copolymers have been matters of keen interest because among all natural biodegradable polymers only PHA polymers possess thermoplastic and mechanical properties similar to those of synthetic polymers [1–10]. Poly[(*R*)-3-hydroxybutyrate] (PHB; Fig. 1) is a natural and biodegradable polyester found in some bacteria as an energy storage system [1–5]. PHB is a very attractive polymer, but it is not always well suited for certain applications as a commodity plastics because of the high stereoregularity of biologically produced macromolecules; PHB is highly crystalline and, hence, too rigid, stiff, and brittle. It has also been known that the mechanical properties of PHB homopolymer films deteriorate markedly after secondary crystallization [11,12]. Accordingly, microbial PHB homopolymer has been regarded as a polymer that must be copolymerized with other monomer components from the viewpoint of industrial applications [13–15].

It has been reported that the copolymerization of a longer side-chain 3-hydroxyhexanoate (3-HHx) comonomer with

* Corresponding author. Research Center for Environment Friendly Polymers, Kwansei Gakuin University, Sanda 669-1337, Japan. Tel.: +81 79 565 8349; fax: +81 79 565 9077.
E-mail address: hsato@ksc.kwansei.ac.jp (H. Sato).

0032-3861/$ - see front matter © 2007 Elsevier Ltd. All rights reserved.
doi:10.1016/j.polymer.2007.03.001

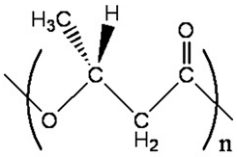

PHB

Fig. 1. Chemical structure of poly(3-hydroxybutyrate) (PHB).

the highly crystalline 3-hydroxybutyrate (3-HB) units significantly reduces the crystallinity and increases the flexibility of PHB [16–18]. The PHB-based copolymers such as poly-[(*R*)-3-hydroxybutyrate-*co*-(*R*)-3-hydroxyhexanoate] (P(HB-*co*-HHx)) show a wide range of physical properties depending on the chemical structure of the comonomer units as well as the comonomer composition.

Another direction of improving the physical properties of PHB is to improve the mechanical properties of PHB films and fibers by preparing uniaxial and biaxial oriented films [6,13,19–23]. Recently, Iwata et al. [6,24–29] succeeded in producing ultra-high-molecular-weight PHB (UHMW-PHB, $M_w = 3.3–14 \times 10^6$) under specific fermentation conditions [28] by using a recombinant *Escherichia coli* XL-1 Blue (pSYL105) bacterium [29] harboring *Ralstonia eutropha* PHB biosynthesis *phbCAB* genes. It has been found that the films of UHMW-PHB can be oriented easily and reproducibly by hot-drawing at a temperature below, but near the crystalline melting point [24,25,29]. The hot-drawn and annealed UHMW-PHB films have high crystallinity and acceptable mechanical properties for industrial and mechanical applications. Iwata et al. [24–26] also prepared cold-drawn and annealed UHMW-PHB films with good mechanical properties and long-term stability by utilizing the PHBs produced by both wild-type and recombinant bacteria. Moreover, they recently reported the first strong PHB fibers processed from UHMW-PHB by cold-drawing and two-step drawing [6,30].

According to recent studies on the X-ray fiber diagrams of highly oriented PHB films and fibers [6,26,27,31], PHB assumes two types of molecular conformations: the 2/1 helix conformation (α-form) [32,33] and the planar zigzag conformation (β-form) [6,26,27,31]. Usually, PHB takes α-form in an orthorhombic system with $a = 5.76$ Å, $b = 13.20$ Å, and $c = 5.96$ Å. In the cell the two antiparallel chains are packed together with the ester group nearly at the same level [32,33]. The chains have left-handed helix and the C=O and CH_3 groups are oriented outside the helix [32,33]. It was recently found that the two-step drawn and annealed film of UHMW-PHB contains β-form as well as α-form [6,26]. β-Form is introduced by the orientation of free chains in the amorphous regions between α-form lamellar crystals, and is responsible for the good mechanical properties of the PHB films and fibers [34,35].

The existence of the β-form seems to be clear from the WAXD studies [25,26], but besides WAXD, no other methods have detected the β-form in the PHB films and fibers; ^{13}C magic-angle spinning (MAS) NMR and differential scanning calorimetry were unsuccessful. Quite recently, Nishiyama et al. [36] reported 2D NMR observation of strain-induced β-form in PHB. The 2D NMR spectra provided the ^{13}C carbonyl signal of β-form separated from that of the 2/1 helix conformation (α-form) and the orientations of the carbonyl carbons for β-form were detected.

The present study is to investigate the formation of β-form in the cold and two-step-drawn films of UHMW-PHB by using IR and Raman spectroscopies and quantum chemical calculations. Until now, we have been investigating structure, crystallinity, and thermal behavior of PHB and P(HB-*co*-HHx) (HHx = 2.5, 3.4, and 12 mol%) by means of wide-angle X-ray diffraction (WAXD) [37,38], infrared (IR) spectroscopy [38–42], quantum chemical calculation [42], and differential scanning calorimetry (DSC) [38]. The present vibrational spectroscopy study provides unambiguous evidences for the existence of the β-form. Raman spectroscopy is useful as a nondestructive and in situ structural analysis technique, and can be applied easily to both thick and thin polymer films. In the present study we made detailed band assignments for Raman spectra of the α- and β-forms based on the quantum chemical calculations of their model compounds. Furthermore, heat-induced degradation from the β-form to an amorphous state is also investigated by using Raman spectroscopy.

2. Experiment

2.1. Preparation of the four kinds of films

Ultra-high-molecular PHB (UHMW-PHB) ($M_w = 5.3 \times 10^6$ and polydispersity = 1.7) was produced by *E. coli* XL-1 Blue containing a stable plasmid pSYL105 harboring *R. eutropha* H16 PHB biosynthesis gene operon *phbCAB*, according to the method reported previously [29].

Solvent-cast films of UHMW-PHB were prepared by a conventional solvent-casting technique from chloroform solutions of polymers. The amorphous preforms of films for preparing a cold-drawn film were produced by melting the solvent-cast films in a hot press at 200 °C and subsequently quenching into ice water. The cold-drawn film was prepared by 1000% stretching of the amorphous preform in ice water. A two-step-drawn film was obtained from further 150% drawing of the cold-drawn film at room temperature. On the other hand, the solvent-cast films were drawn in a silicon oil bath at 165 °C by the loosely-hanging-weights-method to produce a hot-drawn film. All the films, solvent-cast film, cold-drawn film, two-step-drawn film, and hot-drawn film, were annealed in an autoclave at 100 °C for 2 h. The structures of four kinds of films have been confirmed by wide-angle X-ray diffraction, and only two-step-drawn film has a planar zigzag conformation (β-form) together with 2_1 helix conformation (α-form). Other three kinds of films consist only of α-form molecular conformation.

2.2. IR and Raman measurements

IR spectra of the films were measured at a 2 cm^{-1} spectral resolution by using a Thermo Nicolet NEXUS 470 Fourier-transform (FT) IR spectrometer equipped with a liquid

nitrogen-cooled mercury cadmium telluride (MCT) detector. To ensure a high signal-to-noise ratio, 512 scans were co-added. Raman spectra were measured for four kinds of UHMW-PHB films by using a Fourier-transform Raman spectrometer (Thermo Nicolet) with an InGaSb detector. An excitation wavelength at 1064 nm was provided by an Nd:YAG laser, and the laser power at the sample position was typically 200 mW. Raman scattering was collected in a 180° back scattering geometry. The Raman spectra were obtained with a spectral resolution of 4 cm^{-1}, and 1024 scans were co-added to ensure a high signal-to-noise ratio.

2.3. Quantum chemical calculations

The ab initio model calculations were carried out at the density functional theory (DFT, B3LYP functional) and Møller-Plessent (MP2) levels of theory employing the Gaussian 03 program package [43,44]. In the model compound study of the α- and β-structures of PHB we used a single chain octamer model: $HOOC(CH_2CH(CH_3)OCO)_7CH_2CH(CH_3)OH$.

3. Results and discussion

3.1. Raman spectra of four kinds of UHMW-PHB films

Fig. 2 shows Raman spectra in the 1000–400 cm^{-1} region of four kinds of UHMW-PHB. Assignments for major bands in this region are summarized in Table 1. These assignments

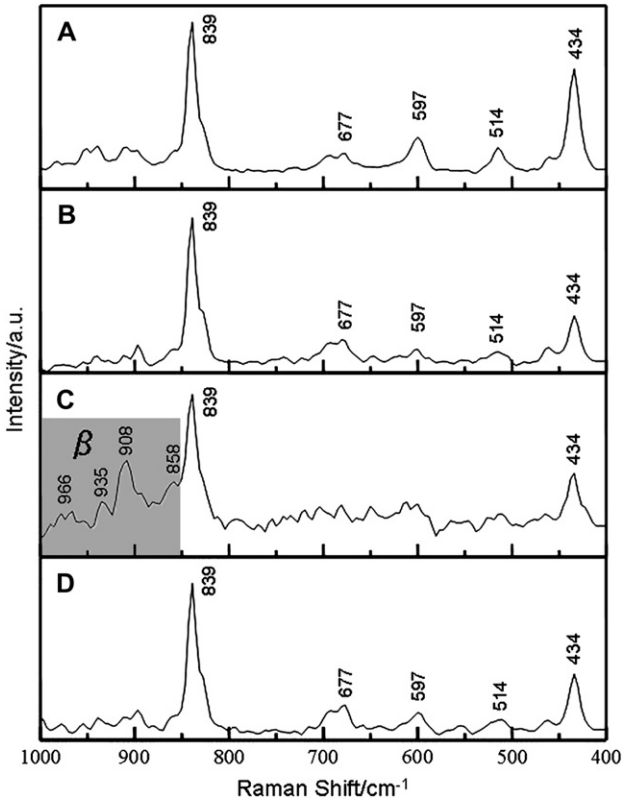

Fig. 2. Raman spectra in the 1000–400 cm^{-1} region of (A) solvent-cast film, (B) cold-drawn film, (C) two-step-drawn film, and (D) hot-drawn film.

Table 1
Observed (sample 2 and sample 3) and calculated wavenumbers (cm^{-1}) of Raman bands of PHB

Wavenumber (cm^{-1})				Assignment
Cold-drawn film	Two-step-drawn film	Calculated α	Calculated β	
1451	1456	1458	1462	CH_3 ab2
1444	1441	1428	1431	CH_2 b
1402	1402	1381	1379	CH_3 sb
1363	1363	1351	1356	CH d, CH_2 w, CH_3 sb
1352	1348	1342	1339	CH d, CH_2 w, CH_3 sb
1292	1298	1277	1295	CH_2 w, CH d, C–CO s, O–CO s
			1286	CH d, O–CO s
		1254		O–CO s, CH_2 t, C–CO s, CH d
1259	1259	1233		CH_2 t, O–CO s, CH d
1220	1226	1196	1214	CH_2 t, C–C s
		1181		CH_2 t, C–C s, O–CO s
			1173	CH_2 w, O–CO s
			1164	O–CO s, CH_2 w
	1131	1113	1126	C–C s, CH_3 r1
1101	1101	1104		CH_3 r1, C–C s, O–C s
		1076	1080	CH_2 t, CH_3 r1
1059	1059	1051	1048	C–O s, CH_2 r1, C–CH_3 s
		1033		C–O s, C–CH_3 s, CH_2 t
	966	959	951	C–CO s, O–C s, C–C s, CH_3 r2
		933		C–CO s, O–C s, CH_3 r2
	935	907	902	CH_3 r2, CH_3 r, C–CH_3 s
		893		CH_3 r2, C–CH_3 s
	908	874	878	CH_3 r2, C–C s
	858		843	CH_3 r2, C–CH_3 s, CH_2 r
839	839	815		C–O s, O–CO s, COC d
		797		O–C s, C–CO s, COC d
		701	711	C=O ip b, COC d, CCC d
677		671	675	C=O opb, CH_2 r, C b
597		625		C=O opb, C–CO s, C b
			564	C=O op b, C–O tor
			527	COC d, CCO d
			508	CCO d, COC d
514		478	475	CCO d, CH_3 r2
		429	416	CCC d, CCO d
434	434	404		CCO d, C b, CO ipb

were based on the quantum chemical calculation of the present study. Of particular note in Fig. 2 is the Raman spectrum of two-step drawn film showing four characteristic bands at 966, 935, 908, and 858 cm^{-1}. The Raman spectra in the 1000–400 cm region of other three films are very close to each other, but the relative intensities of bands at 597 and 434 cm^{-1} relative to that of a band at 839 cm^{-1} change significantly from sample to sample.

In order to make detailed assignments for Raman bands characteristic of two kinds of molecular conformations, we made quantum chemical calculations for the helical structure (α-structure) and the planar zigzag structure (β-structure) of the octamer model. Both models are single chain models. Fig. 1 depicts calculated α- and β-structures for the octamers. Fig. 3 compares Raman spectra in the 1000–400 cm^{-1} region

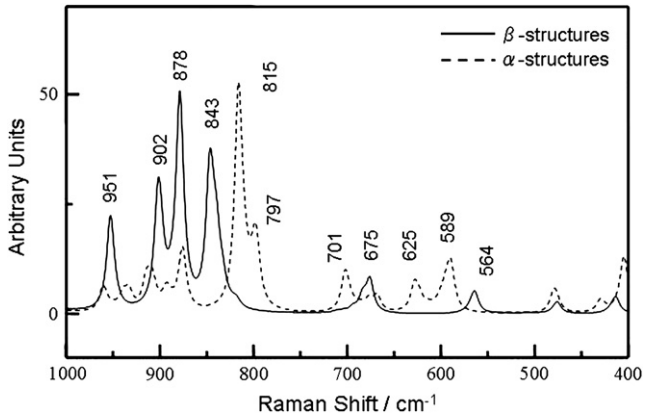

Fig. 3. Raman spectra in the 1000–400 cm^{-1} region of α- and β-structures of the model compound (single chain octamer) calculated by quantum chemical calculations.

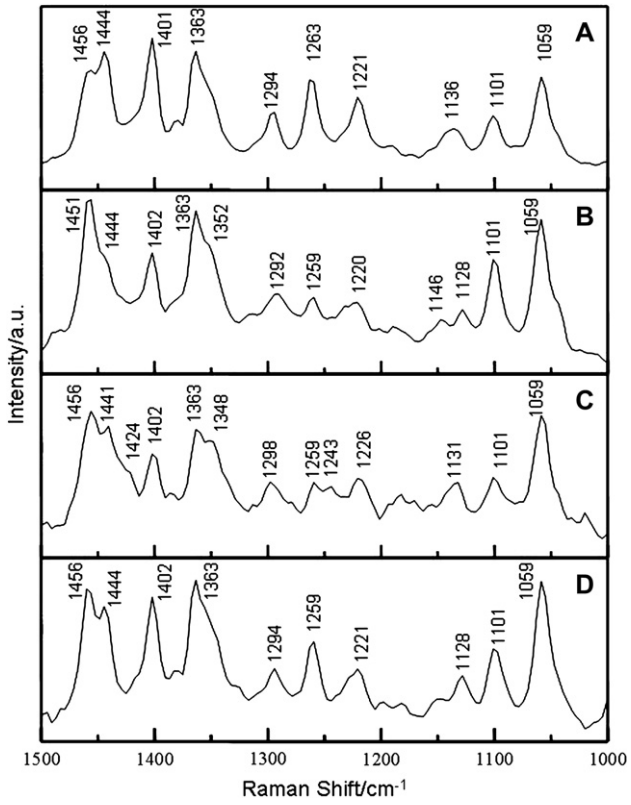

Fig. 4. Raman spectra in the 1500–1000 cm^{-1} region of (A) solvent-cast film, (B) cold-drawn film, (C) two-step-drawn film, and (D) hot-drawn film.

calculated by quantum chemical calculations for both structures. The calculated spectrum of the α-structure is characterized by an intense band at 815 cm^{-1} with a shoulder at 797 cm^{-1}, due to coupling mode of C–O stretching, O–C=O stretching, and C–O–C deformation and that of O–C stretching, C–C–O stretching, and C–O–C deformation, respectively, while the calculated spectrum of the planar zigzag structure shows four characteristic bands at 951, 902, 878, and 843 cm^{-1}. The spectral patterns of the Raman spectra of the three kinds of films except for the two-step-drawn film are very close to that of the calculated spectrum of the helical structure, confirming that these films assume the helical structure. The four characteristic bands at 966, 935, 908, and 858 cm^{-1} of the two-step-drawn film (Fig. 2) are very likely to correspond to the four bands at 951, 902, 878, and 843 cm^{-1} in the calculated spectrum of the planar zigzag structure (β-structure; Fig. 3). It is noted that not only the frequencies but also the relative intensities of the four bands are very close to each other between the observed and calculated spectra. This may be a very strong evidence for the existence of β-structure in the two-step-drawn film. Iwata et al. [6] suggested, based on the reflections on an X-ray fiber diagram of a two-step-drawn film and fiber of UHMW-PHB, that the two-step-drawn film includes the β-form as well as the α-form. Thus, the present Raman result is in good agreement with the X-ray result. Among the three spectra of solvent-cast, cold-drawn and hot-drawn films, the spectrum of cold-drawn film shows a relatively weak band at 434 cm^{-1}. The 434 cm^{-1} band is characteristic of the crystalline state, because the amorphous sample of PHB obtained at a temperature above the melting point does not yield a band at 434 cm^{-1}. Therefore, the crystallinity may be slightly lower in the cold-drawn film.

Fig. 4 displays Raman spectra in the 1500–1000 cm^{-1} region of four kinds of UHMW-PHB films. Band assignments in this region are also shown in Table 1. This region may be divided into three: the 1500–1320 cm^{-1}, 1300–1200 cm^{-1}, and 1200–1000 cm^{-1} regions. The first region contains bands due to the CH_3 and CH_2 bending modes, the second region is concerned mainly with bands arising from the C–O–C stretching modes, and the last region involves mainly C–C stretching bands.

The Raman spectra of solvent-cast and hot-drawn films are very close to each other, however, the Raman spectrum of cold-drawn film is significantly different from those of solvent-cast and hot-drawn films in terms of the weak intensities of bands at 1444, 1402, and 1259 cm^{-1}. These three bands are characteristic of the crystalline state of the helical structure, so that the weak intensities of these three bands suggest that the two-step-drawn film contains more amorphous state than the solvent-cast and hot-drawn films. In the spectrum of two-step-drawn film, the intensities of the bands at 1402 and 1259 cm^{-1} are weak and several additional bands appear at 1424 and 1243 cm^{-1}. According to the quantum calculations, bands each in the 1500–1400 cm^{-1} and 1300–1175 cm^{-1} regions are quite sensitive to the conformations (Table 1). Therefore, the appearances of the additional bands indicate that the two-step-drawn film contains not only α-structure but also β-structure.

Fig. 5 shows Raman spectra in the 1780–1660 cm^{-1} region of four kinds of UHMW-PHB films. We studied temperature-dependent Raman spectral changes for PHB and found that the intensity of a band at 1726 cm^{-1} decreases very gradually from room temperature to ca. 165 °C and decreases rapidly above 165 °C while a broad feature around 1740 cm^{-1} increases largely above 165 °C [43]. Based on these spectral changes and the corresponding spectral variations in an IR spectrum of PHB [37,39], we assigned the bands at 1726 and

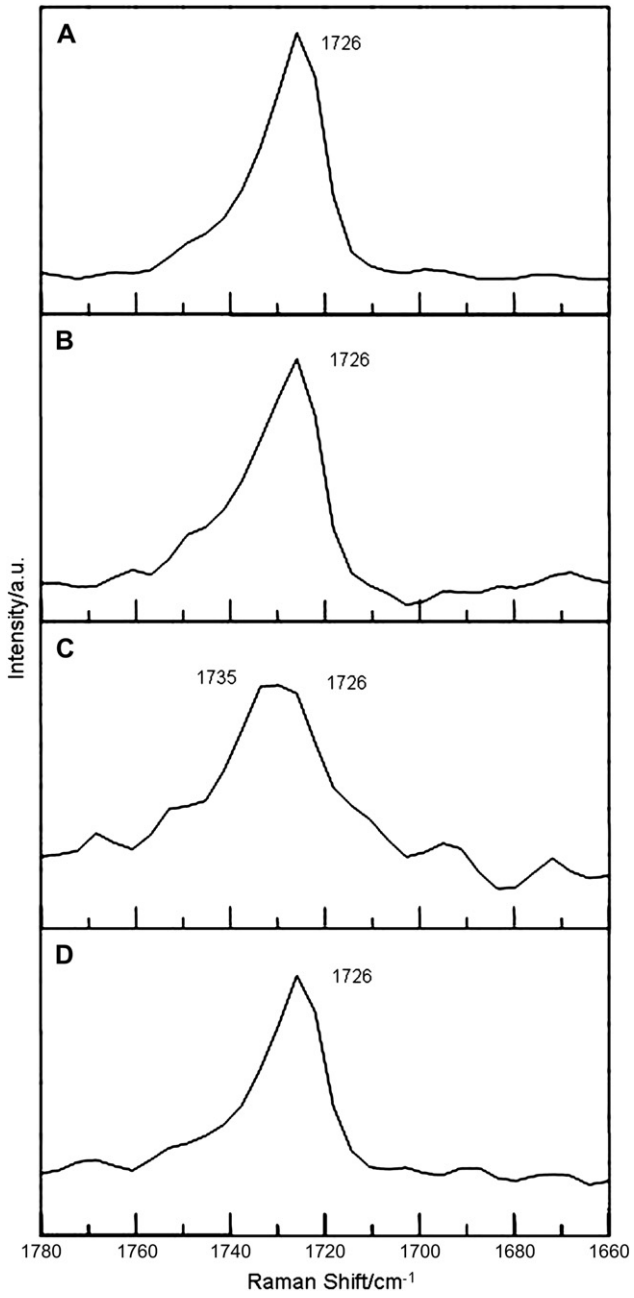

Fig. 5. Raman spectra in the 1780–1660 cm^{-1} region of (A) solvent-cast film, (B) cold-drawn film, (C) two-step-drawn film, and (D) hot-drawn film.

1740 cm^{-1} to the C=O stretching modes of the crystalline and amorphous parts, respectively. It is interesting to note that the crystalline C=O stretching band is broader in the spectrum of two-step-drawn film than in those of solvent-cast and hot-drawn films and that the spectrum of two-step-drawn film shows an additional peak near 1735 cm^{-1}.

The broad feature at 1726 cm^{-1} and more pronounced appearance of a shoulder near 1740 cm^{-1} in the spectrum of cold-drawn film suggest that this film contains more amorphous parts than the solvent-cast and hot-drawn films. The additional band at 1735 cm^{-1} in the spectrum of two-step-drawn film may be another evidence for the existence of β-structure because according to the quantum chemical calculations, the planar zigzag structure of octamer model yields a band near 1735 cm^{-1}.

Fig. 6 exhibits Raman spectra in the 3050–2850 cm^{-1} region of four kinds of UHMW-PHB films. Referring to our previous IR studies [37,39], a weak feature at 3009 cm^{-1} is assigned to a C–H stretching mode of the C–H···C=O hydrogen bonding between the CH_3 group and the C=O group in PHB. The relative intensity of this band is weaker in the spectrum of two-step-drawn film than in those of other three films. It is also noted that a band at 2879 cm^{-1} shifts to a higher wavenumber in the spectrum of two-step-drawn film compared with the corresponding bands of other films. These observations suggest that the two-step-drawn film has more disordered parts than others.

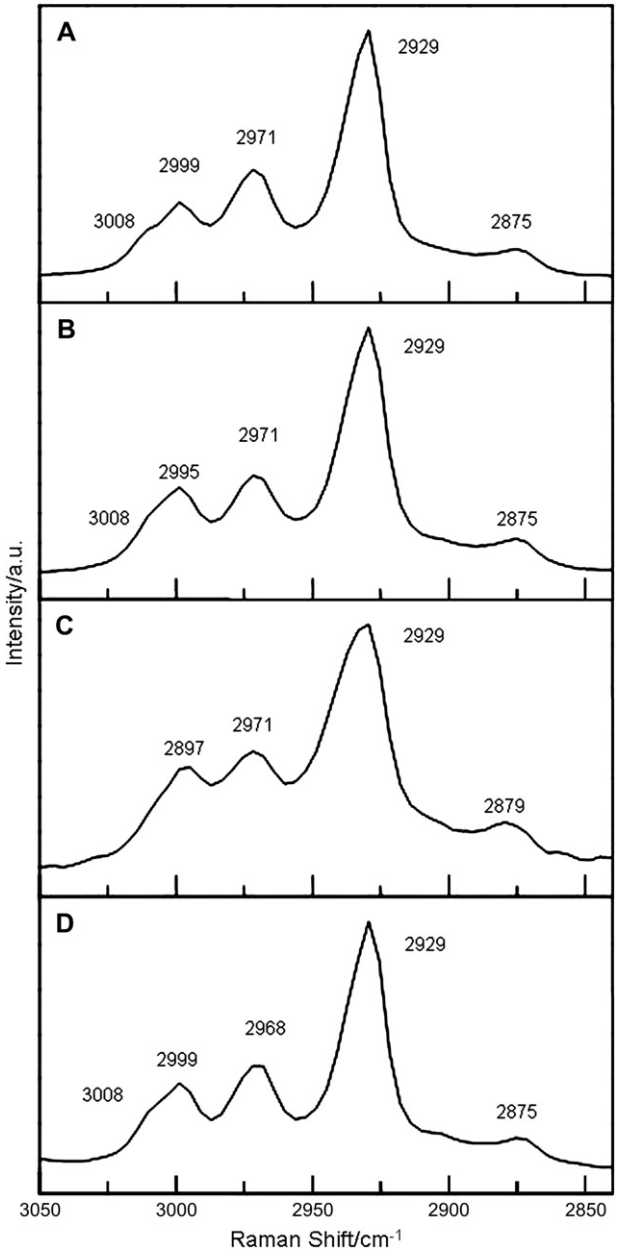

Fig. 6. Raman spectra in the 3050–2850 cm^{-1} region of (A) solvent-cast film, (B) cold-drawn film, (C) two-step-drawn film, and (D) hot-drawn film.

3.2. IR spectra of the four kinds of UHMW-PHB films

Fig. 7 shows IR spectra in the region for the first overtone of the C=O stretching band of the four kinds of UHMW-PHB films. The films prepared were fairly thick, so that we examined the first overtone region of the C=O stretching band instead of the fundamental region where a strong band due to the C=O stretching mode is saturated. It is noted in the overtone region that all the samples show a band at 3436 cm^{-1}. In our previous IR study of spherulite structure of PHB and P(HB-*co*-HHx), we found that they show an intense band at 1723 cm^{-1} due to the C=O stretching mode of the crystalline state [39]. Therefore, the band at 3436 cm^{-1} is assigned to the first overtone of the C=O stretching band of the α crystalline phase. An IR measurement of hot-drawn film at 182 °C revealed that the overtone band due to the amorphous parts appears at 3458 cm^{-1} (data not shown). All the samples show a broad feature near 3460 cm^{-1} assignable to the overtone of the C=O stretching band of the amorphous parts. Of particular interest is that the intensity of the amorphous band is much stronger in the spectrum of two-step-drawn film. Therefore, it seems that the two-step-drawn film contains much more amorphous parts than other samples. We cannot observe a C=O stretching band assignable to the β-form even in the second derivative of the spectrum shown in Fig. 7(C). The C=O band of the β crystalline phase may be obscured in the broad feature in the 3450–3440 cm^{-1} region.

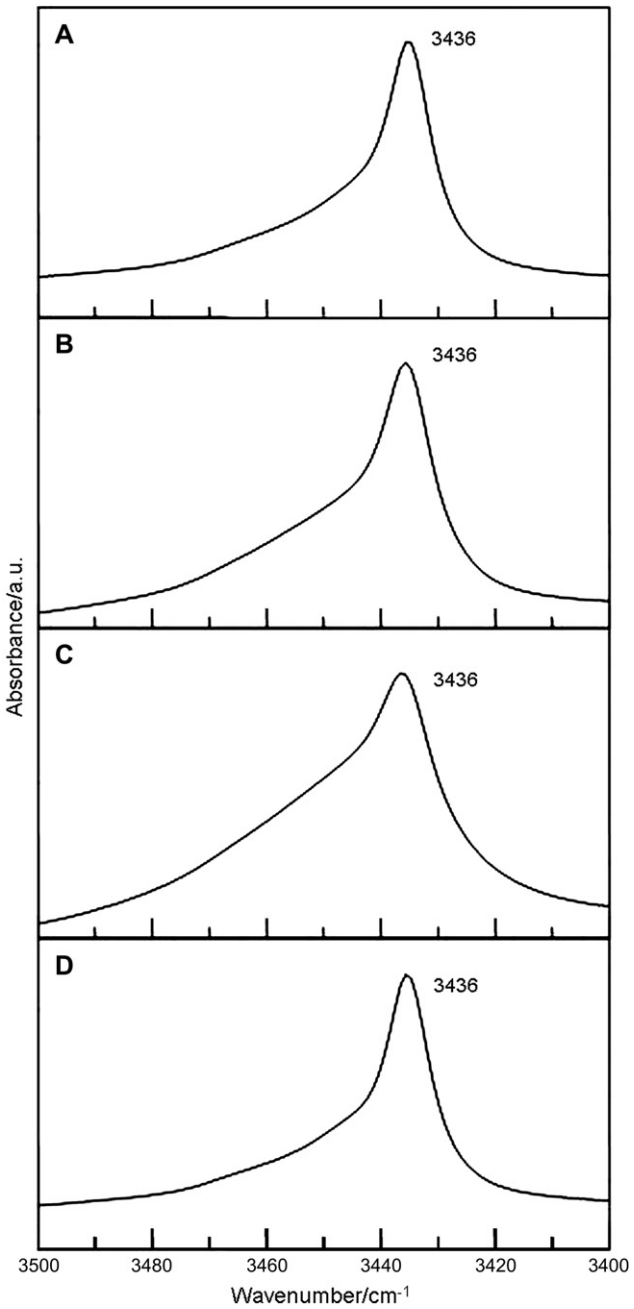

Fig. 7. IR spectra in the 3500–3400 cm^{-1} region of films of (A) solvent-cast film, (B) cold-drawn film, (C) two-step-drawn film, and (D) hot-drawn film at room temperature.

Fig. 8 displays IR spectra in the C–H stretching vibration region of the four kinds of UHMW-PHB films and their second derivatives, respectively. The spectra and their second derivatives of the four films are similar to those of PHB previously reported [39]. We measured IR spectra of PHB over a temperature range of 20 °C–185 °C. Based on the temperature-dependent spectral variations, we made assignments for major IR bands in the CH stretching vibration region. According to our previous study [39], five bands at 3009, 2995, 2984, 2975, and 2967 cm^{-1} in the second derivative spectra may be assigned to the CH_3 asymmetric stretching modes. Only the band at 2984 cm^{-1} increases with temperature; it indicates that the band at 2984 cm^{-1} is due to the CH_3 asymmetric stretching mode of the amorphous parts. The other four bands at 3009, 2995, 2974, and 2967 cm^{-1} are probably due to the CH_3 asymmetric stretching modes of the crystalline parts.

As in the case of Raman spectra (Fig. 6), all the four films yield a band at 3009 cm^{-1} assignable to the C–H stretching band of the C–H···C=O hydrogen bond [37,39]. Therefore, it is very likely that the strength of the C–H···O=C hydrogen bond is nearly the same among the four kinds of films. It is noted in the comparison of the four spectra that the two-step-drawn film shows a relatively strong band at 2984 cm^{-1} due to the amorphous part (Fig. 8(C)). Therefore, this again suggests that two-step-drawn film contains significantly more amorphous parts than other samples. It is also noted that two-step-drawn film has additional bands (shoulder) near 2940 and 2880 cm^{-1} (see Fig. 8(C′)). These bands are also assignable to the amorphous parts. Another important point in Fig. 8 is that the IR spectra of solvent-cast and cold-drawn films show a broad feature near 2985 cm^{-1} due to the amorphous part (Fig. 8(A) and (B)) and that of hot-drawn film gives rise to very weak corresponding feature and shows the clear shoulder at 3009 cm^{-1}. These results suggest that hot-drawn film contains more crystalline parts than the solvent-cast and cold-drawn films.

3.3. Formation and stability of the β-structure in the two-step-drawn film

The results of the Raman and IR spectra clearly show that the two-step-drawn film contains the β-structure. However, it

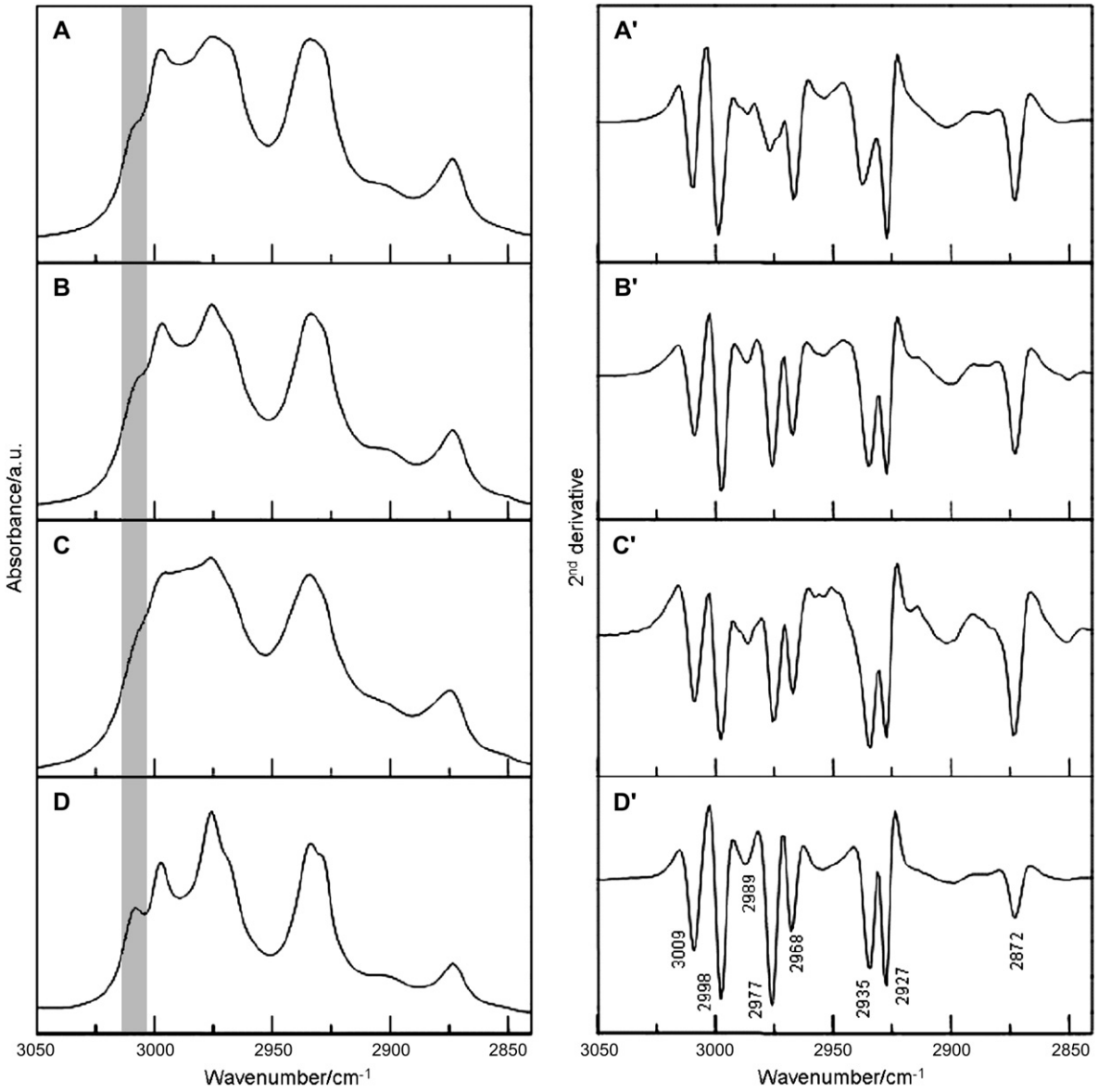

Fig. 8. (A), (B), (C), (D), IR spectra in the 3050–2850 cm^{-1} region of films of solvent-cast film, cold-drawn film, two-step-drawn film, and hot-drawn film at room temperature. (A′), (B′), (C′), (D′), the second derivatives of four spectra (A), (B), (C), and (D).

seems that the amount of β-structure is small because the overall spectral patterns of two-step-drawn film are close to those of α-structure and the relative intensities of the bands arising from the β-structure are weak.

The Raman and IR spectra reveal that the two-step-drawn film contains more amorphous parts than other samples. Thus, it is likely that the crystallinity of the β-structure is rather low. In other words, the β-structure in the two-step-drawn film may have less ordered structure. This calculation is consistent with the result of WAXD by Iwata et al. [29] that the WAXD shows only one strong peak derived from the β-structure in the equatorial line.

In order to explore degradation of the β-structure by heat treatment in the two-step-drawn film, it was heated up to 130 °C, cooled down to room temperature, and then its Raman spectra were measured. Fig. 9 depicts Raman spectra in the 1000–400 cm^{-1}, 1500–1000 cm^{-1}, and 1780–1660 cm^{-1} regions of the two-step-drawn film after the heat treatment. It is noted that the five characteristic Raman bands of the β-structure at 966, 935, 908, 858, and 1738 cm^{-1} disappear in the Raman spectra shown in Fig. 9. These observations suggest that the β-structure disappears after the heat treatment. This disappearance was suggested also by the measurements of WAXD of two-step-drawn film [29]. It can be concluded that the β-form is less stable than the α-form.

4. Conclusions

Based on the Raman and IR spectra of solvent-cast, cold-drawn, two-step-drawn and hot-drawn films of UHMW-PHB and the quantum chemical calculations of α- and β-structures of the single chain model compound (octamer) of PHB, we have reached the following conclusions. (1) The two-step-drawn film contains the β-structure as well as the α-structure.

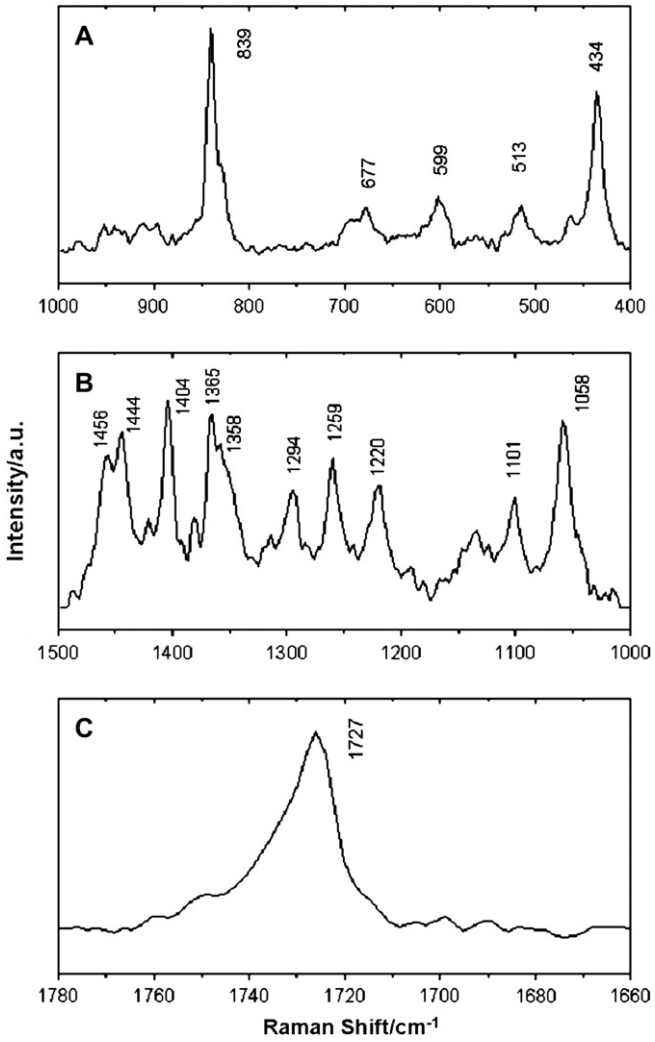

Fig. 9. Raman spectra in the (A) 1000–400 cm^{-1}, (B) 1500–1000 cm^{-1}, and (C) 1780–1660 cm^{-1} region of a two-step-drawn film measured at room temperature after heat treatment up to 130 °C.

The most significant evidence for the existence of β-structure comes from the appearance of the four bands at 966, 935, 908, and 858 cm^{-1} and the additional band at 1735 cm^{-1}. (2) The amount of β-structure in the two-step-drawn film may be small because the intensities of the bands assignable to β-structure are weak. (3) When the two-step-drawn film was heated above 130 °C, the above five bands disappeared, showing that the β-structure is less stable than the α-form.

Acknowledgements

The authors thank Thermo Electron K.K. for measuring the FT–Raman spectra of the five samples. This work was partially supported by ''Open Research Center'' project for private universities: matching fund subsidy from MEXT (Ministry of Education, Culture, Sports, Science and Technology), 2001–2008, Kwansei Gakuin University ''Special Research'' project, 2004–2008, and Grant-in-Aid for Young Science (B) from the Ministry of Education, Culture, Sports, Science and Technology (MEXT) of Japan (No. 18750107). Financial support of the Grant Agency of the Czech Republic (project 203/05/0425) is gratefully acknowledged.

References

[1] Doi Y. Microbial polyesters. New York: VCH Publishers; 1990.
[2] Anderson AJ, Dawes EA. Microbiol Rev 1990;54:450–72.
[3] Chiellini E, Solaro R. Recent advances in biodegradable polymers and plastics. Weinheim: Wiley-VCH; 2003.
[4] Doi Y. ICBP 2003 first IUPAC international conference on bio-based polymers, macromolecular bioscience, vol. 4, issue 3. Weinheim: Wiley-VCH; 2004.
[5] Bastioli C. Handbook of biodegradable polymers. Rapra Technology Limited; 2005.
[6] Iwata T, Aoyagi Y, Fujita M, Yamane H, Doi Y, Suzuki Y. Macromol Rapid Commun 2004;25(11):1100–4.
[7] Satkowski MM, Melik DH, Autran JP, Green PR, Noda I, Schechtman LA. In: Steinbüchel A, Doi Y, editors. Biopolymers. Weinheim: Wiley-VCH; 2001. p. 231.
[8] Yoshie N, Saito M, Inoue Y. Macromolecules 2001;34(26):8953–60.
[9] Doi Y, Kitamura S, Abe H. Macromolecules 1995;28(14):4822–8.
[10] Website: www.nodax.com.
[11] de Koning GJM, Lemstra PJ. Polymer 1993;34(10):4089–94.
[12] Scandola M, Ceccorulli G, Pizzoli M. Macromol Chem Rapid Commun 1989;10:47–50.
[13] Holmes PA. In: Bassett DC, editor. Developments in crystalline polymers, vol. 2. London and New York: Elsevier Applied Science; 1988. p. 1–65.
[14] Nakamura S, Doi Y, Scandola M. Macromolecules 1992;25(17):4237–41.
[15] Pizzoli M, Scandola M, Ceccorulli G. Macromolecules 1994;27(17):4755–61.
[16] Abe H, Doi Y, Aoki H, Akehata T. Macromolecules 1998;31(6):1791–7.
[17] Kobayashi G, Shiotani T, Shima Y, Doi Y. In: Doi Y, Fukuda K, editors. Biodegradable plastics and polymers. Amsterdam: Elsevier; 1994. p. 410.
[18] Kunioka M, Tamaki A, Doi Y. Macromolecules 1989;22(2):694–7.
[19] de Koning GJM, Scheeren AHC, Lemstra PJ, Peeters M, Reynaers H. Polymer 1994;35(21):4598–605.
[20] Barham PJ, Keller A. J Polym Sci Phys Ed 1986;24:69–77.
[21] Gordeyev SA, Nekrasov YP. J Mater Sci Lett 1999;18:1691–2.
[22] Schmack G, Jehnichen D, Vogel R, Tandler B. J Polym Sci Part B Polym Phys 2000;38(21):2841–50.
[23] Yamane H, Terao K, Hiki S, Kimura Y. Polymer 2001;42(7):3241–8.
[24] Kusaka S, Abe H, Lee SY, Doi Y. Appl Microbiol Biotechnol 1997;47:140–3.
[25] Lee SY, Lee KM, Chang HN, Steinbüchel A. Biotechnol Bioeng 1994;44:1337–47.
[26] Kusaka S, Iwata T, Doi Y. Int J Biol Macromol 1999;25:87–94.
[27] Kusaka S, Iwata T, Doi Y. J Macromol Sci Pure Appl Chem 1998;35:319–35.
[28] Aoyagi Y, Doi Y, Iwata T. Polym Degrad Stab 2003;79(2):209–16.
[29] Iwata T, Tsunoda K, Aoyagi Y, Kusaka S, Yonezawa N, Doi Y. Polym Degrad Stab 2003;79(2):217–24.
[30] Tanaka T, Fujita M, Takeuchi A, Suzuki Y, Uesugi K, Ito K. Macromolecules 2006;39(8):2940–6.
[31] Fisher J, Aoyagi Y, Enoki M, Doi Y, Iwata T. Polym Degrad Stab 2004;83(3):453–60.
[32] Yokouchi M, Chatani Y, Tadokoro H, Teranishi K, Tani H. Polymer 1973;14(6):267–72.
[33] Cornibert J, Marchessault HR. J Mol Biol 1972;71(3):735–56.
[34] Orts WJ, Marchessault RH, Bluhm TL, Hamer GK. Macromolecules 1990;23(26):5368–70.
[35] Iwata T, Fujita M, Aoyagi Y, Doi Y, Fujisawa T. Biomacromolecules 2005;6(3):1803–9.
[36] Nishiyama Y, Tanaka T, Yamazaki T, Iwata T. Macromolecules 2006;39(12):4086–92.

[37] Sato H, Mori K, Murakami R, Ando Y, Takahashi I, Zhang J, et al. Macromolecules 2006;39(4):1525–31.
[38] Sato H, Nakamura M, Padermshoke A, Yamaguchi H, Terauchi H, Ekgasit S, et al. Macromolecules 2004;37(10):3763–9.
[39] Sato H, Murakami R, Padermshoke A, Hirose H, Senda K, Noda I, et al. Macromolecules 2004;37(19):7203–13.
[40] Padermshoke A, Katsumoto Y, Sato H, Ekgasit S, Noda I, Ozaki Y. Polymer 2004;45(19):6547–54.
[41] Zhang J, Sato H, Noda I, Ozaki Y. Macromolecules 2005;38(10): 4274–81.
[42] Sato H, Dybal J, Murakami R, Noda I, Ozaki Y. J Mol Struct 2005; 744–747:35–46.
[43] Becke AD. J Chem Phys 1993;98:5648–52.
[44] Frisch MJ, Trucks GW, Schlegel HB, Scuseria GE, Robb MA, Cheeseman JR, et al. Gaussian 03, revision C.02. Wallingford, CT: Gaussian, Inc.; 2004.